Contribution from the Department of Chemistry and Biochemistry, Texas Tech University, Lubbock, Texas 79409, and Department of Chemistry, University of New Orleans, New Orleans, Louisiana 70148

Oxo-Bridged Chromium(III) Dimers Derived from the Reactions of Anions (NCS^-, NCO^-, N_3^-, CN^-, Cl^-) with the Bis(μ-hydroxo)bis{(tris(2-pyridylmethyl)amine)chromium(III)} Ion

Boyd G. Gafford,[†] Charles O'Rear,[†] Jian H. Zhang,[‡] Charles J. O'Connor,[‡] and Robert A. Holwerda*,[†]

Received November 14, 1988

Five linear, oxo-bridged dimers of the form $[L(tmpa)CrOCr(tmpa)L]^{2+}$ (L = NCS^-, NCO^-, N_3^-, CN^-, Cl^-) have been prepared through the nucleophilic displacement of a hydroxo bridge from $[(tmpa)Cr(OH)_2Cr(tmpa)]^{4+}$ by L^-. A mechanism involving the migration of a bridging oxo function to a cis coordination position is proposed to account for the change in stereochemistry that accompanies the conversion of the chromium diol to $[(tmpa)(SCN)CrOCr(NCS)(tmpa)]^{2+}$. Electronic spectra, magnetic susceptibilities, and one-electron-oxidation half-wave potentials of the dimers are reported along with acid ionization constants of the corresponding hydroxo-bridged $[L(tmpa)Cr(OH)Cr(tmpa)L]^{3+}$ complexes. Large singlet–triplet energy gaps determined from the temperature dependence of the magnetic susceptibilities of the oxo-bridged dimers with L = NCS^- (509 cm^{-1}) and CN^- (580 cm^{-1}) support the formulation of diamagnetic ground states with the π electronic configuration $(e_u^b)^4(e_g)^4(b_{2g})^2$, where e_u^b, e_g, and b_{2g} represent the π-bonding level, a nonbonding Cr-centered π MO and a weakly δ-bonding orbital in the approximate D_{4h} symmetry of the $N_5CrOCrN_5$ coordination sphere, respectively. The assignment of two strong $[L(tmpa)CrOCr(tmpa)L]^{2+}$ dimer absorptions near 28 500 and 24 000 cm^{-1} to e_g–e_u^* and b_{2g}–e_u^* transitions (e_u^* designates the π-antibonding level) is supported in part by a study of the e_g–e_u^* band energy dependence on solvent dielectric constant for L = SCN^-. Consistent with expectations from the π molecular orbital model, pK_a values of the hydroxo-bridged complexes fall off sharply with increasing $10Dq$ while $E_{1/2}$ for the $[L(tmpa)CrOCr(tmpa)L]^{2+/3+}$ couple follows an increasing trend as the L^- substituent moves from weaker to stronger fields within the spectrochemical series.

Introduction

Subsequent to the serendipitous discovery of the (μ-oxo)bis{pentaaquachromium(III)} (aqua dimer) ion in 1980,[1] we have pursued the synthesis of an extensive family of linear, oxo-bridged Cr(III) dimers with the objective of correlating electronic structure with redox and substitutional reactivities. Thus far, the molecular orbital treatment[2] of the distinctive bonding in oxo-bridged dimers, based on M(dπ)–O(pπ)–M(dπ) orbital overlaps, has proved to be useful in understanding reductant[3] and anion[4] catalysis of aqua dimer acid hydrolysis to $Cr(H_2O)_6^{3+}$ and the unusually facile loss of ammonia from $[(NH_3)_5Cr]_2O^{4+}$ (basic rhodo ion) to give $[(NH_3)_5Cr(OH)Cr(NH_3)_4(OH)]^{4+}$ (rhodo erythro ion).[5] Hydroxo bridge displacement from $[(tmpa)Cr(OH)_2Cr(tmpa)]^{4+}$ (tmpa = tris(2-pyridylmethyl)amine) by nucleophiles[6] provided a precedent for the synthesis of Cr^{III}–O–Cr^{III} dimers with variations in both aromatic amine and complementary monodentate ligands. We report here the synthesis and physical characterization of five complexes having the general formula $[L(tmpa)CrOCr(tmpa)L]^{2+}$, where L = SCN^-, N_3^-, NCO^-, CN^-, and Cl^-. Syntheses of two analogous $[L(bpy)_2CrOCr(bpy)_2L]^{2+}$ complexes (L = SCN^- and N_3^-) are also described. Of particular interest in this paper is the mechanism of bridging OH^- displacement from $[(tmpa)Cr(OH)_2Cr(tmpa)]^{4+}$ by monodentate incoming groups; X-ray crystallographic evidence for L = SCN^-[6] indicates that the apical tmpa N atoms originally trans relative to the Cr_2O_2 core of the diol[7,8] are both trans to thiocyanate N atoms in the oxo-bridged dimer.

Experimental Section

Materials. Reagent grade chemicals and doubly or triply distilled water were used throughout. The preparations of $[(tmpa)Cr(OH)_2Cr(tmpa)](ClO_4)_4\cdot 4H_2O$[7] (**1**), $[(tmpa)Cr(OH)OCr(tmpa)](ClO_4)_3\cdot H_2O$[7] (**2**), $[(bpy)_2Cr(OH)_2Cr(bpy)_2](ClO_4)_4\cdot 2H_2O$[6] (**3**), and $[(tmpa)(SCN)CrOCr(NCS)(tmpa)](ClO_4)_2\cdot 0.5H_2O$[6] (**4**) (IR: ν_{as}(CrOCr) = 858 cm^{-1}; ν(CN) = 2053 cm^{-1}) have already been described. Yields of **4** obtained from the reactions of **1** with NaSCN in pure water and dilute perchloric acid (pH 3.5) were found to be identical (60%). Spectrophotometric Cr and C, H, N microanalyses were obtained as before.[7] *Caution!* Although no problem has been encountered in handling the perchlorate salts described in this work, the potential explosion hazard should be noted, particularly when grinding crystals into powders and working with the compounds at elevated temperatures.

$[(tmpa)(N_3)CrOCr(N_3)(tmpa)](ClO_4)_2\cdot 2H_2O$ (5). **1** (1.00 g, 0.841 mmol) was ground to a fine powder, dried at 100 °C for 30 min, and then dissolved in 150 mL of hot CH_3CN. When NaN_3 (1.092 g, 16.8 mmol) was added and the mixture was refluxed for 2 h, the color of the solution changed from purple to deep green. After the solution was cooled and filtered to remove excess NaN_3, ether was added slowly with stirring until a precipitate formed. The dark green product was then collected in 73% yield by filtration and air-dried. Anal. Calcd for $[(tmpa)(N_3)CrOCr(N_3)(tmpa)](ClO_4)_2\cdot 2H_2O$: Cr, 10.2; C, 42.41; H, 3.95; N, 19.23. Found: Cr, 10.0; C, 42.65; H, 3.73; N, 18.79. IR: ν_{as}(CrOCr) = 865 cm^{-1}; ν(NN) = 2061 cm^{-1}.

$[(tmpa)(OCN)CrOCr(NCO)(tmpa)](ClO_4)_2$ (6). **1** (1.00 g, 0.841 mmol) was dissolved in 100 mL of hot acetonitrile, the solution combined with 1.36 g (16.8 mmol) of KOCN, and the mixture refluxed for 2 h. The brown-green product was precipitated by slow ether addition after removal of excess KOCN by filtration. Crude **6** was then recrystallized three times by dissolving in 700 mL of doubly distilled H_2O, slowly adding solid $LiClO_4$ with stirring until precipitation commenced, and then allowing the solid to digest at 5 °C for 4 h. The final crop (87% yield) of dark green crystals was washed with water and air-dried. Anal. Calcd for $[(tmpa)(OCN)CrOCr(NCO)(tmpa)](ClO_4)_2$: Cr, 10.6; C, 46.40; H, 3.69; N, 14.24. Found: Cr, 10.2; C, 46.32; H, 3.71; N, 14.21. IR: ν_{as}(CrOCr) = 873 cm^{-1}; ν(CN) = 2210 cm^{-1}.

$[(tmpa)(NC)CrOCr(CN)(tmpa)](ClO_4)_2\cdot 2H_2O$ (7). **1** (1.00 g, 0.841 mmol) was dissolved in 100 mL of hot CH_3CN, the solution was mixed with 0.825 g (16.8 mmol) of NaCN, and the mixture was refluxed for 2 h. Following removal of excess NaCN from the cooled mixture by filtration, the brown-green product was isolated after the addition of 10.0 g of $LiClO_4$ and 50 mL of H_2O and slow evaporation of CH_3CN until precipitation was complete. One recrystallization was performed by dissolving the solid in the minimum amount of H_2O at room temperature and then adding $LiClO_4$ with stirring. **7** (81% final yield) was filtered, washed with water, and air-dried. Anal. Calcd for $[(tmpa)(NC)CrOCr(CN)(tmpa)](ClO_4)_2\cdot 2H_2O$: Cr, 10.5; C, 46.21; H, 4.08; N, 14.18. Found: Cr, 10.7; C, 46.11; H, 3.64; N, 14.02. IR: ν_{as}(CrOCr) = 865 cm^{-1}; ν(CN) = 2120 cm^{-1}.

$[Cl(tmpa)CrOCr(tmpa)Cl](ClO_4)_2\cdot 2H_2O$ (8). **1** (1.00 g, 0.841 mmol) was ground to a fine powder, dried at 100 °C for 30 min, and then combined with 0.983 g (16.8 mmol) of NaCl in 100 mL of hot CH_3CN. After it was refluxed for 1 h, the solution was cooled, filtered, and transferred to a large beaker. Ether was slowly added with stirring until a brown-green precipitate was seen. The product (95% yield) was iso-

[†] Texas Tech University.
[‡] University of New Orleans.

(1) Holwerda, R. A.; Petersen, J. S. *Inorg. Chem.* **1980**, *19*, 1775.
(2) Dunitz, J. D.; Orgel, L. E. *J. Chem. Soc.* **1953**, 2594.
(3) Johnston, R. F.; Holwerda, R. A. *Inorg. Chem.* **1985**, *24*, 3176.
(4) Johnston, R. F.; Holwerda, R. A. *Inorg. Chem.* **1985**, *24*, 3181.
(5) Gafford, B. G.; Holwerda, R. A. *Inorg. Chem.* **1988**, *27*, 210.
(6) Gafford, B. G.; Holwerda, R. A.; Schugar, H. J.; Potenza, J. A. *Inorg. Chem.* **1988**, *27*, 1126.
(7) Gafford, B. G.; Holwerda, R. A. *Inorg. Chem.* **1989**, *28*, 60.
(8) Hodgson, D. J.; Zietlow, M. H.; Pedersen, E.; Toftlund, H. *Inorg. Chim. Acta* **1988**, *149*, 111.

0020-1669/89/1328-1720$01.50/0

lated by filtration, washed with ether, and air-dried. Recrystallization from water was not feasible because **8** rapidly decays to **1** in this solvent. Anal. Calcd for $[Cl(tmpa)CrOCr(tmpa)Cl](ClO_4)_2 \cdot 2H_2O$: Cr, 10.3; C, 42.96; H, 4.00; N, 11.13. Found: Cr, 10.4; C, 42.76; H, 3.60; N, 10.96. IR: $\nu_{as}(CrOCr) = 844\ cm^{-1}$.

$[Cr(tmpa)Cl_2](ClO_4) \cdot 2.5H_2O$ (9). **1** (1.00 g, 0.841 mmol) was converted to $Cr(tmpa)(OH_2)_2^{3+}$ in 100 mL of water as before,[7] followed by saturation of the solution with NaCl and heating at 60 °C for 3 h. The large dark red crystals of **9** that formed upon overnight refrigeration of the product solution (70% yield) were washed with cold triply distilled water and air-dried. Anal. Calcd for $[Cr(tmpa)Cl_2](ClO_4) \cdot 2.5H_2O$: Cr, 9.3; C, 40.06; H, 3.92; N, 10.38. Found: Cr, 9.4; C, 40.02; H, 3.67; N, 10.26. UV–vis (H_2O; λ_{max} (ϵ_{max})): 395 nm (127 $M^{-1}\ cm^{-1}$), 539 nm (122 $M^{-1}\ cm^{-1}$).

$[(bpy)_2(SCN)CrOCr(NCS)(bpy)_2](ClO_4)_2 \cdot H_2O$ (10). **3** (4.00 g, 3.34 mmol) was dissolved in 300 mL of boiling water and then combined with 10.8 g (134 mmol) of NaSCN. The color of the solution changed from red-brown to dark chocolate brown within 30 s, when crystalline **10** began to form. The reaction mixture was allowed to boil for an additional 10 min, at which time the solid was isolated by filtering the hot solution, washed with water, and air-dried. The dark chocolate brown microcrystals (58% yield) showed no change in percent Cr upon recrystallization from water. Anal. Calcd for $[(bpy)_2(SCN)CrOCr(NCS)(bpy)_2](ClO_4)_2 \cdot H_2O$: Cr, 9.6; C, 46.80; H, 3.18; N, 12.99. Found: Cr, 9.6; C, 46.81; H, 2.91; N, 12.83. IR: $\nu_{as}(CrOCr) = 856\ cm^{-1}$; $\nu(CN) = 2066\ cm^{-1}$. UV–vis (CH_3CN; λ_{max} (ϵ_{max})): 301 nm (52 300 $M^{-1}\ cm^{-1}$).

$[(bpy)_2(N_3)CrOCr(N_3)(bpy)_2](ClO_4)_2 \cdot H_2O$ (11). **3** (1.00 g, 0.836 mmol) was mixed with 2.17 g (33.4 mmol) of NaN_3 in 100 mL of boiling water. After several minutes, the color of the solution changed from red to dark brown, but unlike the preparation of **10**, no precipitate emerged. $LiClO_4$ (5.0 g) was then added to the hot solution, inducing the precipitation of the chocolate brown product within 2–3 min. **11** was isolated by filtration of the hot solution, washed with water, and air-dried. The crude product was recrystallized by dissolving in 200 mL of acetone and adding 2.00 g of $LiClO_4$ dissolved in 20 mL of H_2O, followed by slow evaporation. The crystals (23% yield) that formed upon reducing the solution volume to 30 mL were washed with water and air-dried. Anal. Calcd for $[(bpy)_2(N_3)CrOCr(N_3)(bpy)_2](ClO_4)_2 \cdot H_2O$: Cr, 9.9; C, 45.94; H, 3.28; N, 18.75. Found: Cr, 9.9; C, 46.58; H, 3.03; N, 18.79. IR: $\nu_{as}(CrOCr) = 836\ cm^{-1}$; $\nu(NN) = 2059\ cm^{-1}$. UV–vis (λ_{max} (ϵ_{max})): 300 nm (56 000 $M^{-1}\ cm^{-1}$).

Physical Measurements. UV–visible and infrared spectra (KBr pellets) were acquired on Shimadzu UV-260 and Perkin-Elmer Model 1600 spectrophotometers, respectively. In order to determine the acid ionization constants of $[L(tmpa)Cr(OH)Cr(tmpa)L]^{3+}$ complexes, spectrophotometric titrations (25.0 °C, I = 0.1 M ($NaNO_3$)) were carried out on buffered (10 mM) aqueous solutions over the pH 1–10 range,[7] absorbance being monitored at the most intense near-ultraviolet transition (near 350 nm) and nonlinear least-squares fits of the absorbance, $[H^+]$ data to the appropriate expression for a single-step ionzation[9] being performed. Electrochemical measurements were made at a Pt-button working electrode with a Bioanalytical Systems CV-1B triangular wave generator, with use of the electrode configuration, methods, and conditions described previously.[6]

Preliminary magnetic measurements at ambient temperature were performed on a Johnson-Matthey magnetic susceptibility balance, calibrated against $Hg[Co(SCN)_4]$. Magnetic susceptibility temperature dependence data were recorded with a SHE Corp. VTS superconducting SQUID susceptometer. The sample bucket was fabricated from an Al–Si alloy obtained from SHE Corp. The magnetic susceptibility of the sample bucket was measured independently over the temperature region of 6–300 K, and the magnetic data for all samples were then corrected for the bucket contribution. All of the samples were examined at a field of 5 kOe. Measurement and calibration procedures are described elsewhere.[10] Magnetic susceptibilities corrected for diamagnetism by using Pascal's constants are expressed per dimer unit (i.e. two Cr ions per molecule) as a function of temperature. The model of an isolated Heisenberg dimer containing $S = {}^3/_2$ ions with interaction Hamiltonian $\mathbf{H} = -2J\mathbf{S}_1 \cdot \mathbf{S}_2$ was used to analyze the data for binuclear compounds, **1**, **2**, **4**, and **7**. The susceptibility (χ') based on this model is[10]

$$\chi' = \frac{Ng^2\mu_B^2}{kT} \frac{2e^{2J/kT} + 10e^{6J/kT} + 28e^{12J/kT}}{1 + 3e^{2J/kT} + 5e^{6J/kT} + 7e^{12J/kT}} \quad (1)$$

where all of the parameters have their usual meaning. Taking into account the possibility of monomeric impurities that obey the Curie–Weiss expression, the magnetic data were fit to relationship 2 by a nonlinear least-squares procedure that weights the data so that the percent difference deviation is minimized; ρ and Θ represent the impurity fraction and the Weiss constant, respectively.

$$\chi_m = \chi'(1 - \rho) + Ng^2\mu_B^2 S(S + 1)\rho/3k(T - \Theta) + TIP \quad (2)$$

Results

Synthesis of $[L(tmpa)CrOCr(tmpa)L]^{2+}$ and Related bpy Complexes. The preparations of $[L(tmpa)CrOCr(tmpa)L]^{2+}$ (L = SCN^-, NCO^-, CN^-, N_3^-, and Cl^-) by displacement of a single hydroxo bridge from $[(tmpa)Cr(OH)_2Cr(tmpa)]^{4+}$ according to reaction 3 proceed with excellent yields. Although the thiocyanate

$$[(tmpa)Cr(OH)_2Cr(tmpa)]^{4+} + 2L^- \rightarrow [L(tmpa)CrOCr(tmpa)L]^{2+} + H_2O \quad (3)$$

complex was prepared in a boiling aqueous solution,[6] better yields are generally obtained from refluxing acetonitrile, even though Na^+ or K^+ salts of the L^- ligands are only slightly soluble in this medium. The dimers with L = N_3^- and Cl^- cannot be isolated from aqueous solutions at all, owing to dimer cleavage (N_3^-) or diol regeneration (Cl^-) side reactions. Indeed, the success of the aqueous synthetic route depends on the precipitation of the CrOCr dimer prior to the onset of decomposition side reactions.

Not all anions examined gave linear, oxo-bridged products when refluxed with **1** in CH_3CN. Thus, NaF and $Na(CH_3CO_2)$ gave excellent yields of $[(tmpa)Cr(O)(F)Cr(tmpa)]^{3+}$ and $[(tmpa)Cr(O)(CH_3CO_2)Cr(tmpa)]^{3+}$,[11] respectively, while treatment of the diol with sodium pyrazolate or sodium imidazolate afforded quantitative yields of ionization product **2**. The comparison of halide ion reactions with **1** is particularly intriguing, since F^- gives an oxo fluoro, doubly bridged product and Cl^- induces the formation of an oxo-bridged dimer, while Br^- and I^- fail to react with the diol.

Interestingly, all attempts to prepare $[L(tmpa)CrOCr(tmpa)L]^{4+}$ species from reactions of the diol with neutral monodentate ligands such as ammonia, pyridine, and *N,N*-dimethylformamide have failed, in both aqueous and acetonitrile solutions. Thus, the first two potential incoming groups quantitatively remove a proton from **1** to give **2**, which is inert to further reaction. Acetonitrile solutions of the diol are unchanged upon refluxing for 12 h in the presence of a 10-fold excess of dmf or equimolar pyridine and pyridinium perchlorate. At this point, it is not clear whether the failure to isolate $[L(tmpa)CrOCr(tmpa)L]^{4+}$ complexes reflects a thermodynamic or a kinetic barrier to reaction 3.

X-ray diffraction analysis of $[(tmpa)(SCN)CrOCr(NCS)(tmpa)](SCN)_2$ showed that the cation is centrosymmetric with a Cr–O bond length of 1.800 Å, a distorted-octahedral N_5O coordination sphere, and a pronounced lengthening of the Cr–N bond trans to the bridging oxo group (2.12 Å) as compared with the average of the other Cr–pyridyl N bond lengths (2.07 Å).[6] Although X-ray crystallographic structural confirmation is not yet available for any of the other compounds described here, the presence of a linear CrOCr bridge in **4–8**, **10**, and **11** is clearly revealed by distinctive strong asymmetric CrOCr stretching[12,13] infrared bands near 850 cm^{-1} in all cases and the close correspondence between calculated and observed elemental analyses. The strong resemblance of UV–visible spectra, protonation characteristics, and electrochemical profiles among compounds **4–8** (vide infra) further supports their assignment to a common structural class, particularly considering that doubly bridged[7,11] and monomeric[7] $(tmpa)Cr^{III}$ species exhibit very different physical properties. It should be noted, however, that the physical char-

(9) Clemmer, J. D.; Holwerda, R. A. *Inorg. Chem.* **1982**, *21*, 2103.
(10) O'Connor, C. J. *Prog. Inorg. Chem.* **1982**, *29*, 203.
(11) Gafford, B. G.; Holwerda, R. A. Work in progress. The formulations of these mixed-bridge binuclear complexes are based on elemental analyses of perchlorate salts plus spectroscopic, magnetic, and electrochemical measurements, which will be reported separately. Anal. Calcd for $[(tmpa)Cr(O)(F)Cr(tmpa)](ClO_4)_3 \cdot 0.5H_2O$: Cr, 10.1; C, 42.09; H, 3.63; N, 10.91. Found: Cr, 10.0; C, 42.01; H, 3.82; N, 10.88. Calcd for $[(tmpa)Cr(O)(CH_3CO_2)Cr(tmpa)](ClO_4)_2$: Cr, 9.83; C, 43.14; H, 3.72; N, 10.59. Found: Cr, 9.72; C, 43.09; H, 3.61; N, 10.44.
(12) Hewkin, D.; Griffith, W. *J. Chem. Soc. A* **1966**, 472.
(13) Nakamoto, K. *Infrared Spectra of Inorganic and Coordination Compounds*, 2nd ed.; Wiley: New York, 1970.

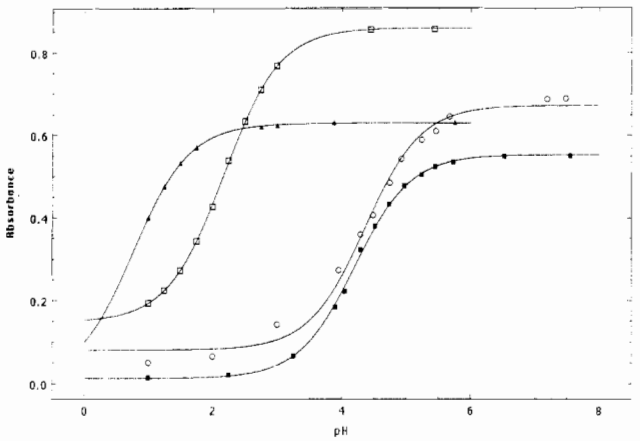

Figure 1. Spectrophotometric titrations of $[L(tmpa)CrOCr(tmpa)L]^{2+}$ complexes with L = CN^- (▲, 0.0493 mM, 354 nm), NCS^- (□, 0.121 mM, 352 nm), NCO^- (○, 0.0493 mM, 347 nm), and N_3^- (■, 0.0667 mM, 351 nm) at 25.0 °C, I = 0.1 M ($NaNO_3$), and 1-cm path length. Solid curves and pK_a values were calculated on the basis of nonlinear least-squares fits (see text).

acterization offered here is not sufficient to prove that all of the L^- donors adopt the trans stereochemistry relative to the CrOCr axis that is preferred by NCS^-.

Electronic Spectroscopy and Ionization Constant Determinations. Electronic spectra of dimers **4–8** in acetonitrile solution (Table I; see ref 6 for the full spectrum of **4**) exhibit a common intense ($\epsilon \approx 10^4$ M^{-1} cm^{-1}), sharp band in the 349–355-nm interval coupled with a second, poorly resolved feature near 420 nm ($\epsilon \approx 3 \times 10^3$ M^{-1} cm^{-1}). Unfortunately, these dominant bands prevent the resolution of d–d transitions, which appear as shoulders between 440 and 460 nm and plateaus with shallow maxima in the vicinity of 570 nm. Both of the dominant near-ultraviolet bands exhibit apparent splittings into components separated by approximately (1–2) × 10^3 cm^{-1}. In the case of the dimer with the least symmetric ligand field, $[Cl(tmpa)CrOCr(tmpa)Cl]^{2+}$, maxima were resolved at {23 800, 25 700} and {27 800, 28 600} cm^{-1} for all four components of the split principal transitions.

Spectrophotometric titrations of **4–7** (Figure 1) revealed that the oxo-bridged dimers accept one proton to give purple $[L(tmpa)Cr(OH)Cr(tmpa)L]^{3+}$ conjugate acids, which exhibit pK_a values that are highly sensitive to the nature of the L group (Table I), reminiscent of rhodo erythro cation acid–base characteristics.[14] The electronic spectra of these protonation products (Table I) lack the intense near-ultraviolet bands of the oxo-bridged precursors, exhibiting only comparatively weak d–d bands and a SCN^--to-Cr(III) LMCT band at 327 nm similar to that reported for $[Cr(tmpa)(NCS)_2]^+$[7] in the case of the thiocyanate complex. All of the hydroxo-bridged $(tmpa)Cr^{III}$ dimers are stronger acids than $[(NH_3)_5Cr]_2(OH)^{5+}$ (acid rhodo ion, pK_a = 7.63)[9] by 3–7 orders of magnitude, which is contrary to expectations on the basis of charge separation considerations alone.

In order to probe the possibility that the strongest near-ultraviolet band of $[L(tmpa)CrOCr(tmpa)L]^{2+}$ dimers corresponds to a metal-to-bridging-oxygen charge-transfer transition, the transition energy for $[(tmpa)(SCN)CrOCr(NCS)(tmpa)]^{2+}$ was determined in 13 solvents and plotted as a function of $(1 - D_{op})/(2D_{op} + 1)$ according to the method of Meyer and co-workers;[15] D_{op} represents the optical dielectric constant of the solvent, computed as the squared value of the refractive index from sources tabulated in ref 15. Spectra were found to be invariant with time, demonstrating that **4** is inert to NCS^- substitution and bridge-cleavage reactions in all solvents considered. Given that the ground state of the oxo-bridged dimer does not have a permanent dipole moment[6] and assuming that the 355-nm (CH_3CN) band is, in fact, a MLCT transition, a plot of band energy vs $(1 - D_{op})/(2D_{op} + 1)$ is expected to be linear with a slope of μ^2/b^3, where μ and b are the dipole moment of the excited state and the radius of the chromophore, treated as a nonpolarizable sphere, respectively.[15] The alternative assignment of this band as a LMCT or MLCT transition involving the tmpa ligand may be dismissed in view of its absence in the spectra of $[Cr(tmpa)Cl_2]^+$ and related monomeric $(tmpa)Cr^{III}$ complexes.[7]

As is shown in Figure 2, the plot of band energy vs $(1 - D_{op})/(2D_{op} + 1)$ for **4** is reasonably linear, with a slope of 4460 ± 410 cm^{-1} and a correlation coefficient of 0.995, confirming the MLCT assignment of the transition. Considering only the N and O donor atoms to be contained within the chromophore sphere (excluding the full pyridyl rings), b is estimated at 3.9 Å from the sum of Cr–O and average Cr–N bond lengths.[6] On this basis, the excited-state dipole moment and dipole length are estimated at 7.3 ± 0.5 D and 1.5 ± 0.2 Å, respectively. Considering the highly approximate nature of this calculation,[15] the close agreement between the Cr–O bond length of 1.8 Å and dipole length computed from the solvent dependence of the absorption spectrum supports the assignment of the dominant near-ultraviolet bands of dimers **4–8** to a transition exhibiting substantial Cr(III)-to-bridging-O MLCT character.

Table I. Physical Properties of $[L(tmpa)CrOCr(tmpa)L]^{2+}$ Complexes

L	UV–vis λ_{max}, nm (ϵ_{max}, M^{-1} cm^{-1})[a] CrOCr dimer[d]	Cr(OH)Cr dimer[e]	pK_a[b]	$E_{1/2}$, V vs SHE[c]
NCS^-	313 (10 800) 355 (14 100) 368 sh (11 200) 398 sh (2750) 417 (2740) 457 sh (1780) 567 pl (250)	327 (8700) 524 (410)	2.05	1.17
NCO^-	308 sh (6750) 349 (10 500) 362 sh (8500) 393 (2980) 420 (3200) 450 sh (2100) 572 pl (200)	403 (180) 533 (340)	4.09	1.02
CN^-	313 sh (6750) 355 (12 800) 367 (11 400) 398 (3050) 414 (2900) 450 sh (1950) 570 pl (230)	510 (230)	0.64	1.17
N_3^-	294 sh (6900) 354 (8600) 364 sh (7650) 416 sh (2350) 448 sh (1730) 572 pl (260)	412 (240) 545 (430)	4.25	0.96
Cl^-	310 sh (5700) 350 (9000) 360 (7950) 389 (2600) 420 (2700) 440 sh (2010) 570 (160)		unstable in water	1.03

[a] Spectra recorded at ambient temperature. Extinction coefficients are expressed per mole of dimer. Intense characteristic tmpa pyridyl π–π^* transition in the 250–260-nm interval is not tabulated. [b] pK_a of conjugate acid $[L(tmpa)Cr(OH)Cr(tmpa)L]^{3+}$ in water at 25.0 °C and I = 0.1 M. Uncertainty estimated at ±0.05. [c] Half-wave potential for the $[L(tmpa)CrOCr(tmpa)L]^{2+/3+}$ oxidation couple in CH_3CN at 25.0 °C and I = 0.1 M TBAP. Uncertainty estimated at ±0.01 V. [d] $[L(tmpa)CrOCr(tmpa)L]^{2+}$ spectrum in CH_3CN solution. [e] $[L(tmpa)Cr(OH)Cr(tmpa)L]^{3+}$ spectrum in 1.0 M aqueous $HClO_4$ except in the case of L = N_3^- (1.0 M $HClO_4$ in 50:50 H_2O–CH_3CN).

Electrochemical Measurements. Consistent with our previous report of a reversible one-electron-oxidation wave for **4** with $E_{1/2}$

(14) Schwarzenbach, G.; Magyar, B. *Helv. Chim. Acta* **1962**, *45*, 1425.
(15) Kober, E. M.; Sullivan, B. P.; Meyer, T. J. *Inorg. Chem.* **1984**, *23*, 2098.

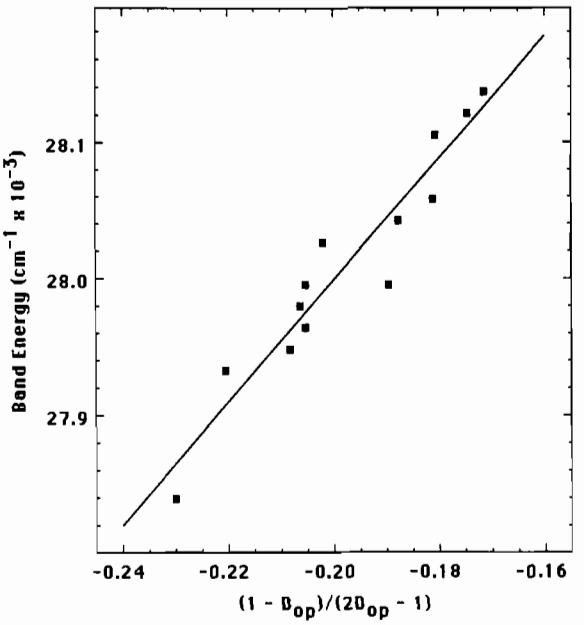

Figure 2. Linear least-squares correlation of $[(tmpa)(NCS)CrOCr(NCS)(tmpa)]^{2+}$ e_g–e_u* transition energy with solvent optical dielectric constant function at ambient temperature. Solvents (band energy x10^{-3} cm^{-1}, $(1 - D_{op})/(2D_{op} + 1)$): methanol (28.14, −0.1714); acetonitrile (28.12, −0.1746); *N*-methylformamide (27.98, −0.2063); dimethyl sulfoxide (27.93; −0.2205); ethanol (28.06, −0.1811); *N*,*N*-dimethylformamide (28.00, −0.2053); *N*,*N*-dimethylacetamide (27.95, −0.2082); propylene carbonate (28.03; −0.2019); acetone (28.11, −0.1806); *N*-methylacetamide (27.96, −0.2053); pyridine (27.84, −0.2300); methyl ethyl ketone (28.04, −0.1876); *n*-butyronitrile (28.00, −0.1895).

Table II. Magnetic Characteristics of Binuclear $(tmpa)Cr^{III}$ Compounds[a,b]

	1	2	4	7
g	1.93	2.16	2.15	2.12
J, cm^{-1}	−15.7	−68.5	−255	−290
zJ',[c] cm^{-1}	3.5	7.2	0	0
TIP, cgsu	0	3.8×10^{-4}	1.7×10^{-5}	4.0×10^{-4}
% impurity with Curie–Weiss behavior	0	0.15	0.09	0.99
Θ	0	−0.936	−0.008	0.252

[a] See Experimental Section for identification of compound numbers. [b] Molecular field corrections for **4** and **7**; TIP, % impurity, and Θ for **1** fixed to 0. [c] Molecular field correction.

= 1.17 V vs SHE,[6] the cyclic voltammograms of all five $[L(tmpa)CrOCr(tmpa)L]^{2+}$ complexes in acetonitrile solution (0.1 M $(n\text{-}Bu)_4NClO_4$ supporting electrolyte) exhibit this feature in the 0.96–1.17-V interval (Table I) with peak-to-peak separations of 70–75 mV at a sweep rate of 50 mV/s and anodic to cathodic peak current ratios (within experimental error) of 1.0. A coulometric determination at a constant working electrode potential 0.3 V more positive than $E_{1/2}$ showed that $n = 0.93 \pm 0.05$ for **4**. Although these $[L(tmpa)CrOCr(tmpa)L]^{2+}$ oxidation waves are fully reversible on the cyclic voltammetric time scale of 10–60 s, it was not possible to isolate the presumed mixed-valence $Cr^{III}OCr^{IV}$ oxidation product of **4** subsequent to a bulk electrolysis experiment which required greater than 1 h to complete. The fate of this product remains under investigation.

Magnetic Properties. Parameters derived from least-squares fits of χ', T points to eq 1 for compounds **1**, **2**, **4**, and **7**[16] are summarized in Table II. Comparisons of experimental points with calculated lines for dependences of the magnetic susceptibilities of **1**, **2**, and **4** on temperature are shown in Figures 3–5, respectively. In each case, the Heisenberg exchange model provides an adequate basis for the quantitative understanding of the temperature-dependence data. The singlet–triplet separation for diol **1** implied by our findings ($-2J = 31.4$ cm^{-1}) agrees well with that published by Hodgson and co-workers (30.58 cm^{-1})[8] while the present work was in progress. This value is similar to those reported for other diols with aromatic amine ligands,[17] $[(bpy)_2Cr(OH)_2Cr(bpy)_2](ClO_4)_4 \cdot 3H_2O$ (37.41 cm^{-1}) and $[(phen)_2Cr(OH)_2Cr(phen)_2](ClO_4)_4 \cdot 2H_2O$ (44.87 cm^{-1}), but is

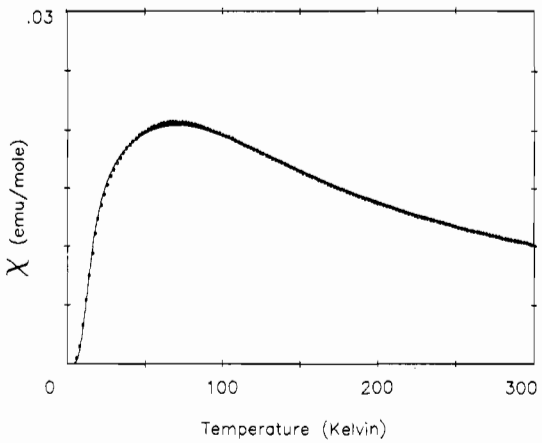

Figure 3. Temperature dependence of the magnetic susceptibility of **1**. The experimental data are shown as dots, and the best fit to eq 2 is drawn as the solid curve. See Table II for nonlinear least-squares magnetic parameters.

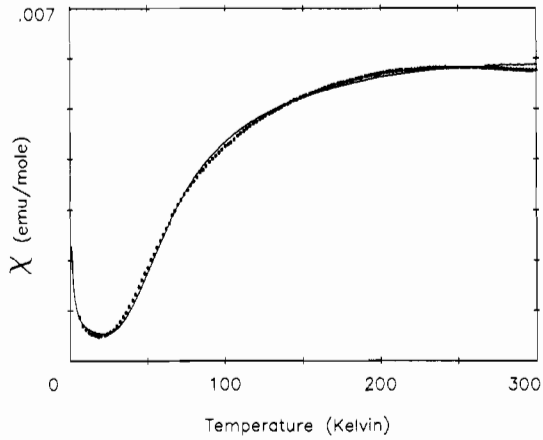

Figure 4. Temperature dependence of the magnetic susceptibility of **2**. The experimental data are shown as dots, and the best fit to eq 2 is drawn as the solid curve. See Table II for nonlinear least-squares magnetic parameters.

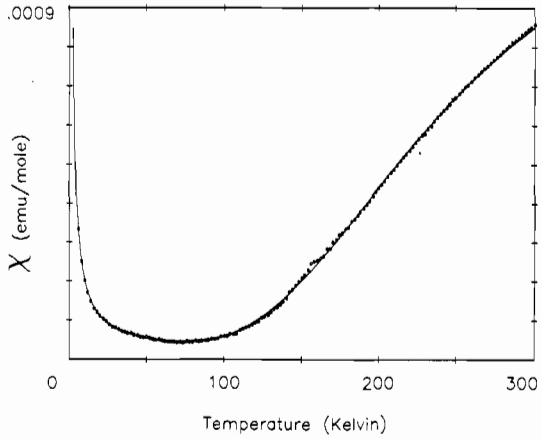

Figure 5. Temperature dependence of the magnetic susceptibility of **4**. The experimental data are shown as dots, and the best fit to eq 2 is drawn as the solid curve. See Table II for nonlinear least-squares magnetic parameters.

(16) The original data for the dependence of compound **7** magnetic susceptibility on temperature may be found in Supplementary Table I.

(17) Josephson, J.; Pedersen, E. *Inorg. Chem.* **1977**, *16*, 2534.

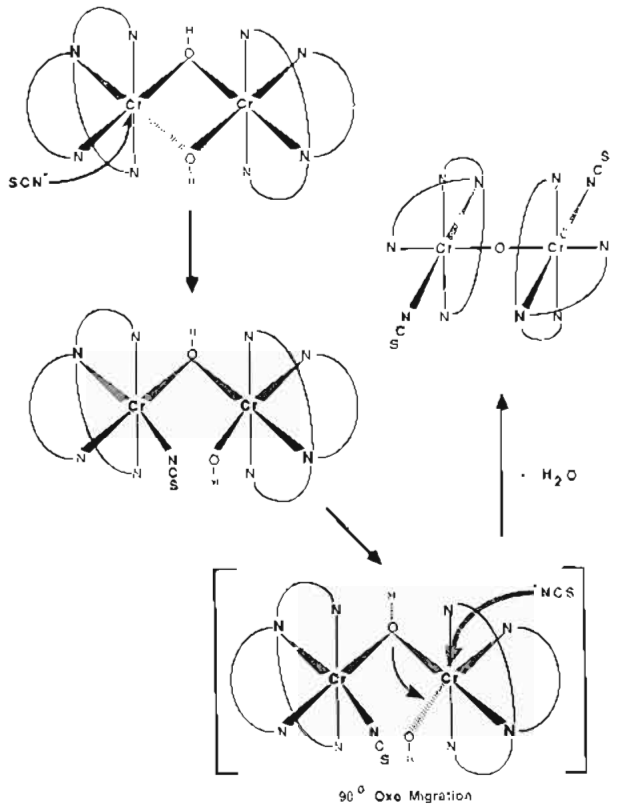

Figure 6. Proposed oxo bridge migration mechanism for the generation of **4** from the reaction of NCS^- with diol **1**.

characteristically larger than singlet–triplet gaps for bis(hydroxo)-bridged dimers with aliphatic amine donor sets.[18] Although the singlet–triplet separation in the tmpa chromium diol is somewhat smaller than those of the analogous phen and bpy systems, the $-2J$ value of 137 cm^{-1} for **2** is substantially larger than the splittings of $[(bpy)_2Cr(OH)OCr(bpy)_2](ClO_4)_3 \cdot 4H_2O$ (60 cm^{-1}) and $[(phen)_2Cr(OH)OCr(phen)_2](ClO_4)_3 \cdot 2H_2O$ (90 cm^{-1}).[17] The presence of strong antiferromagnetic coupling between the Cr atoms of linear, oxo-bridged dimers **4** and **7**, mediated by $d\pi(Cr)-p\pi(O)$, orbital overlaps, is reflected in considerably larger singlet–triplet gaps of 509 and 580 cm^{-1}, respectively, on the same order as that reported for the basic rhodo ion (450 cm^{-1}).[19] Perchlorate, bromide, and nitrate salts of $[(tmpa)(SCN)CrOCr(NCS)(tmpa)]^{2+}$ all exhibited 300 K μ_{eff} values of 0.8 ± 0.1 μ_B, corresponding to approximately 0.3 unpaired electron per chromium atom. No signal could be detected in EPR measurements (Varian E-109 spectrometer) on **4** at ambient and liquid-nitrogen temperatures.

Discussion

Although not completely general, our approach to the synthesis of oxo-bridged chromium(III) dimers through the nucleophilic displacement of a single bridging OH^- group from a diol with aromatic amine ligands has thus far been successful in generating five $[L(tmpa)CrOCr(tmpa)L]^{2+}$ complexes and several similar dimers derived from the bpy and phen diols.[11] The stereochemistry of reactant (**1**) and product (**4**) complexes for $L = SCN^-$ provides an important clue to the mechanism of reaction 3. A rearrangement of tmpa pyridyl N donor arms or migration of the bridging oxo function must take place in order for the apical N atoms of **1** that are each trans to a bridging OH^- group to both adopt positions trans to thiocyanate ligands in **4**. Figure 6 illustrates the sequence of steps that is thought to occur in the conversion of the tmpa diol to an oxo-bridged product in the presence of thiocyanate ion. The initial Cr–OH bond-breaking step, induced by the first L^- incoming group, is analogous to the well-documented ring-opening–ring-closing equilibria of ammonia and ethylenediamine diols.[20,21] In order to achieve the observed product geometry, the remaining bridging oxygen atom must migrate to a cis coordination position concurrent with or prior to nucleophilic attack by the second L^- unit. It is anticipated that rate studies of reaction 3 with various incoming groups will clarify the precise role of this second L^- ion, if any, in promoting the bridging group migration step and release of H_2O. The mechanistic alternative to oxygen bridge migration, cleavage and reformation of all four Cr–N bonds on one chromium center, is considered to be highly unlikely. Continuing mechanistic studies are directed toward the detailed understanding of reaction 3 and the question of whether the failure of neutral incoming groups to generate oxo-bridged dimers from the tmpa diol has a thermodynamic or a kinetic basis.

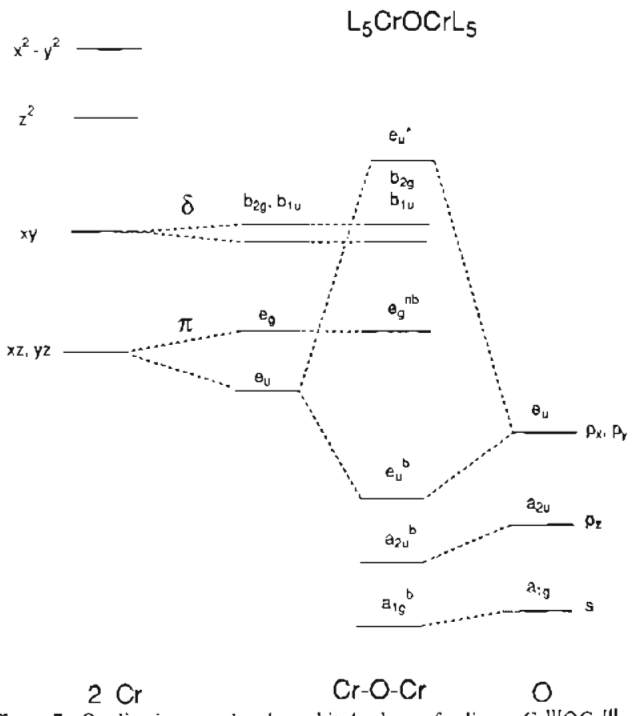

Figure 7. Qualitative π molecular orbital scheme for linear $Cr^{III}OCr^{III}$ dimers, adapted from ref 32. Symmetry labels are based on the hypothetical D_{3h} point group.

The need to formulate the linear MOM unit as an electronically unique moiety, with distinctive properties unexpected for weakly coupled monomers, is apparent from physical measurements on a variety of binuclear transition-metal complexes.[22-31] Considering only π bonding of the $M(d\pi)-O(p\pi)-M(d\pi)$ type, the one-electron molecular orbital scheme proposed originally by Dunitz and Orgel[2] and subsequently applied to the basic rhodo ion by Schmidtke[32]

(18) Hodgson, D. In *Magneto-Structural Correlations in Exchange Coupled Systems*; Willet, R. D., Ed.; Reidel: Dordrecht, The Netherlands, 1985; p 497.
(19) Pedersen, E. *Acta Chem. Scand.* **1972**, *26*, 333.
(20) Christensson, F.; Springborg, J. *Acta Chem. Scand., Ser. A* **1982**, *36*, 21.
(21) Springborg, J.; Toftlund, H. *Acta Chem. Scand., Ser. A* **1976**, *30*, 171.
(22) Cotton, F. A.; Najjar, R. C. *Inorg. Chem.* **1981**, *20*, 1866.
(23) Chakravarty, A. K.; Cotton, F. A. *Inorg. Chem.* **1984**, *23*, 409.
(24) Weaver, T. R.; Meyer, T. J.; Adeyami, S. A.; Brown, G. M.; Eckberg, R. P.; Johnson, E. C.; Murray, R. W.; Untereckер, D. *J. Am. Chem. Soc.* **1975**, *97*, 3039.
(25) Baumann, J. A.; Meyer, T. J. *Inorg. Chem.* **1980**, *19*, 345.
(26) Gilbert, J. A.; Eggleston, D. S.; Murphy, W. R.; Geselowitz, D. A.; Gersten, S. W.; Hodgson, D. J.; Meyer, T. J. *J. Am. Chem. Soc.* **1985**, *107*, 3855.
(27) Doppelt, P.; Meyer, T. J. *Inorg. Chem.* **1987**, *26*, 2027.
(28) Schugar, H. J.; Rossman, G. R.; Barraclough, C. G.; Gray, H. B. *J. Am. Chem. Soc.* **1972**, *94*, 2683.
(29) (a) Campbell, J. R.; Clark, R. J. H. *Mol. Phys.* **1978**, *36*, 1133. (b) Campbell, J. R.; Clark, R. J. H. *J. Chem. Soc., Faraday Trans. 2* **1980**, *76*, 1103.
(30) Glerup, J. *Acta Chem. Scand.* **1972**, *26*, 3775.
(31) DiVaira, M.; Mani, F. *Inorg. Chem.* **1984**, *23*, 409.
(32) Schmidtke, H.-H. *Theor. Chim. Acta* **1971**, *20*, 92.

(Figure 7) is a useful starting point in correlating the spectral, magnetic, electrochemical, and acid–base properties of the oxo-bridged chromium(III) dimers reported in this paper. Considering the CrOCr unit to define the z coordinate axis in the D_{4h} point group of a $N_5CrOCrN_5$ species, e_u^b and e_u^* bonding and antibonding molecular orbitals, respectively, are derived from p_x, p_y (O) and d_{xz}, d_{yz} (Cr) atomic orbitals. The ordering of approximately nonbonding b_{2g}, b_{1u} (derived from d_{xy}) and e_g ($d_{xz,yz}(1) + d_{xz,yz}(2)$ combinations) levels is not easily defined, being dependent on the magnitudes of the tetragonal crystal field component, M–M δ bonding, and π interactions with nonbridging ligands.[2,32-34] Alternative electronic structures[32,35] suggested for $[(NH_3)_5Cr]_2O^{4+}$ include $(e_u^b)^4(e_g)^4(b_{2g})^1(b_{1u})^1$ and $(e_u^b)^4(b_{2g})^2(b_{1u})^2(e_g)^2$.

The properties of $[L(tmpa)CrOCr(tmpa)L]^{2+}$ complexes are entirely consistent with the π molecular orbital model, provided that the predominant electronic structures are $(e_u^b)^4(e_g)^4(b_{2g})^2$ (ground state) and $(e_u^b)^4(e_g)^4(b_{2g})^1(b_{1u})^1$ (first excited state). The exceptionally large singlet–triplet gaps calculated from the magnetic susceptibilities of **4** and **7** clearly point to diamagnetic ground states for both dimers. By comparison with the most intense electronic spectral features of other MOM complexes,[29] the strong, sharp bands of $[L(tmpa)CrOCr(tmpa)L]^{2+}$ ions near 350 nm are most logically assigned to the fully allowed e_g–e_u^* ($^1A_{2u} \leftarrow {}^1A_{1g}$) transition, which has the elements of both a Cr-to-Cr and a Cr-to-O charge-transfer process. Indeed, the solvent dependence of the **4** electronic spectrum supports the attribution of this most intense feature to a MLCT band linked to the central CrOCr chromophore. The appearance of a shoulder toward lower energy on the ~350-nm bands is as expected from the lower (approximately C_{2h}) symmetry of the complexes under consideration, which would lift the degeneracy of both the e_g ($b_g + b_g$) and e_u ($b_u + b_u$) molecular orbitals and give rise to several closely spaced spectral components. The second, less intense band at lower energy in the spectra of **4–8** (398 and 417-nm features of **4**; peaks or shoulders in the 416–420- and 389–398-nm intervals of all complexes) most likely is the b_{2g}–e_u^* ($^1E_u \leftarrow {}^1A_{1g}$) electronic transition.[29] In agreement with this perspective on band assignments is the observation that the splittings of both low- and high-energy electronic transitions are best resolved, as distinct peaks at 350, 360, 389, and 420 nm, for the dimer that exhibits the largest deviation from D_{4h} symmetry, $[Cl(tmpa)CrOCr(tmpa)Cl]^{2+}$. Finally, it should be noted that the remarkable constancy of the e_g–e_u^* band energy among the five $[L(tmpa)CrOCr(tmpa)L]^{2+}$ complexes (28 400 ± 200 cm^{-1} average) agrees with Schmidtke's angular overlap analysis,[32] which expresses the difference in one-electron energies of the e_g and e_u^* molecular orbitals ($\Delta E(e_g–e_u^*)$) according to eq 4, where $e^M{}_{\pi Op}$ and $e_{\pi M}$

$$\Delta E(e_g–e_u^*) = e^M{}_{\pi Op} - 2e_{\pi M} \quad (4)$$

represent the MOM and MM π-bonding energies, respectively. Variations in MOM π-bonding energy with changing L group should be paralleled by the M–M π-overlap energy, such that $\Delta E(e_g–e_u^*)$, which is sensitive to the difference between the two π-bonding energies, will be relatively invariant.

In contrast to the electrochemistry of $[(H_2O)_5Cr]_2O^{4+}$, which exhibits an irreversible one-electron-reduction wave ($E_{1/2}$ = 0.52 V vs SHE) and a susceptibility to reductant-catalyzed acid hydrolysis,[3] the $[L(tmpa)CrOCr(tmpa)L]^{2+}$ complexes are characterized by fully reversible, one-electron-oxidation waves between 0.96 and 1.17 V vs SHE. In spite of its drastically different ligand field, the aqua dimer nevertheless exhibits prominent near-ultraviolet absorption bands close to those observed for the tmpa oxo-bridged dimers (347 nm, $\epsilon = 1.0 \times 10^4$ M^{-1} cm^{-1} per dimer; 413 nm, $\epsilon = 4.6 \times 10^3$ M^{-1} cm^{-1} per dimer) plus an additional strong transition at 443 nm ($\epsilon = 6.0 \times 10^3$ M^{-1} cm^{-1} per dimer) that is not seen in the tmpa CrOCr system.[1] In order to reconcile these observations, we propose that the aqua dimer electronic

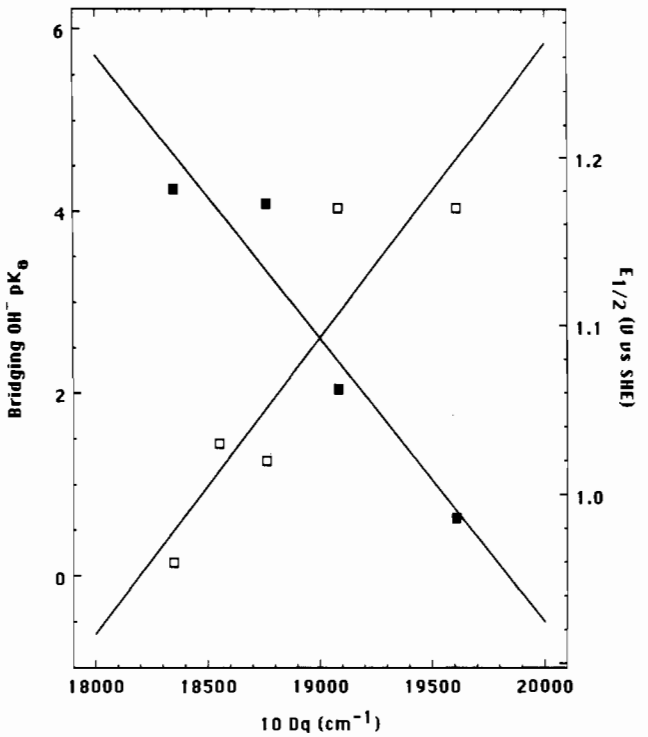

Figure 8. Correlation of $[L(tmpa)Cr(OH)Cr(tmpa)L]^{3+}$ pK_a values (■, left-hand axis) and $[L(tmpa)CrOCr(tmpa)L]^{2+}$ oxidation $E_{1/2}$ values (□, right-hand axis) with $10Dq$ for the hydroxo-bridged dimer. Solid lines represent linear least-squares fits. Since $10Dq$ for $[Cl(tmpa)Cr(OH)Cr(tmpa)Cl]^{3+}$ could not be measured directly (decomposition to **1** in aqueous solution), the value for $[Cr(tmpa)Cl_2]^+$ (18 550 cm^{-1}) is used as an approximation in the $E_{1/2}$ correlation. See Table II for the original data.

configuration is $(e_u^b)^4(b_{2g})^2(b_{1u})^2(e_g)^2$, such that the HOMO's of the tmpa and aqua dimers would be b_{2g} and e_g, respectively. On this basis, a one-electron reduction of the aqua dimer would generate an e_g^3 configurtion that would be subject to Jahn–Teller configurational instability, while one-electron oxidations of the tmpa dimers would leave an $(e_u^b)^4(e_g)^4(b_{2g})^1$ electronic configuration that would not trigger such a distortion. Both complexes should exhibit e_g–e_u^* and b_{2g}–e_u^* electronic transitions, but only the aqua dimer could also have a e_u^b–e_g band, suggesting a possible assignment of its 443-nm feature.

As anticipated from a comparison of basic rhodo and acid rhodo chromium dimer spectra,[36] the presumably bent[37] $[L(tmpa)Cr(OH)Cr(tmpa)L]^{3+}$ protonation products of complexes **4–7** are characterized by UV–visible spectra containing only relatively weak d–d bands and, in the case of L = SCN^-, a thiocyanate LMCT transition. Because the d–d bands of the oxo-bridged dimers are not well resolved, the lowest energy visible transitions of the corresponding hydroxo-bridged complexes may be used to estimate the crystal field parameter $10Dq$. Since π-bonding strength within the CrOCr structural unit is expected to increase with decreasing ΔE(d–p), the energy difference between overlapping Cr 3d and O 2p orbitals, $e^M{}_{\pi Op}$, should also become larger with increasing $10Dq$, given that the d_{xz} and d_{yz} orbitals derived from the octahedral t_{2g} set are specifically implicated in CrOCr π-bonding. Considering that π-bonding strength within a linear, oxo-bridged binuclear complex is not easily assessed by direct measurement, we have probed this important characteristic indirectly through measurements of Cr(OH)Cr complex acid ionization constants. Assuming that the inductive influences of the various L substituents on pK_a are small and that the solvation free energies of the hydroxo-bridged dimers are comparable, pK_a is expected to increase with *decreasing* π-bonding strength within

(33) Jezowska-Trzebiatowska, B. *Pure Appl. Chem.* **1971**, *27*, 89.
(34) Mealli, C.; Sacconi, L. *Inorg. Chem.* **1982**, *21*, 2870.
(35) Earnshaw, A.; Lewis, J. *J. Chem. Soc.* **1961**, 396.
(36) Dubicki, L.; Martin, R. L. *Aust. J. Chem.* **1970**, *23*, 215.
(37) Veal, J. T.; Jeter, D. Y.; Hempel, J. C.; Eckberg, R. P.; Hatfield, W. E.; Hodgson, D. J. *Inorg. Chem.* **1973**, *12*, 2928.

a $[L(tmpa)CrOCr(tmpa)L]^{2+}$ complex. If this is looked at from another perspective, a CrOCr dimer with strong π-bonding will resist protonation, leading to a bent hydroxo-bridged product in which such π-bonding is much weaker or is totally absent.

Figure 8 displays correlations of Cr(OH)Cr dimer acid ionization constants and $[L(tmpa)CrOCr(tmpa)L]^{2+/3+}$ oxidation half-wave potentials with $10Dq$, estimated as the energy of the Cr(OH)Cr dimer $^4T_{2g} \leftarrow {}^4A_{2g}$ (O_h) transition. Consistent with expectations from the π molecular orbital model, pK_a values fall off sharply with increasing $10Dq$ while $E_{1/2}$ generally follows an increasing trend as the L^- substituent moves from weaker to stronger field within the spectrochemical series. The latter observation follows from the expected enhancement of $E_{1/2}$ with decreasing energy of the redox electron,[38] which is ionized from the b_{2g} (essentially nonbonding d_{xy} (t_{2g})) molecular orbital according to our model. Thus, the relationship of electrochemical potentials to t_{2g} orbital and valence state ionization energies is well established for monomeric transition-metal redox couples.[38] From this perspective, $E_{1/2}$ values of the $[L(tmpa)CrOCr(tmpa)L]^{2+}$ complexes are not expected to correlate with the π-bonding energy of the CrOCr unit but rather more simply with $10Dq$, which may be expressed in crystal field terms as the energy difference between $d_{x^2-y^2}$ and d_{xy} orbitals (in point group D_{4h}).[32]

It should be noted that the least-squares lines in Figure 8 are not intended to imply that linear relationships between pK_a or $E_{1/2}$ values and $10Dq$ are anticipated on theoretical grounds. Rather, we are content to establish that quantitative dependences of the dimer physical parameters on $10Dq$ do in fact exist and are reasonable on the basis of a molecular orbital description of the CrOCr bonding. In order to better understand the physical properties of oxo-bridged Cr(III) dimers, it will be necessary to introduce systematic perturbations into the energies of the e_g, b_{2g}, and b_{1u} molecular orbitals, which are not actually nonbonding but may interact with the low-lying π^* levels of phen and bpy aromatic amine ligands, both of which are far better π-acids than the nonconjugated tmpa pyridyl groups. Toward this end, we report here the syntheses of the first two members of the $[L(bpy)_2CrOCr(bpy)_2L]^{2+}$ family but will reserve comment on their characteristics until continuing work on this system has progressed further.

Acknowledgment is made to the donors of the Petroleum Research Fund, administered by the American Chemical Society, and to the Robert A. Welch Foundation (Grant D-735) for their generous support of this research. We also thank Professor John Kenney of Eastern New Mexico University for helpful discussions of the spectroscopic data.

Supplementary Material Available: A listing of the magnetic susceptibilities of dimer **7** as a function of temperature (1 page). Ordering information is given on any current masthead page.

(38) van Gaal, H. L. M.; van der Linden, J. G. M. *Coord. Chem. Rev.* **1982**, *47*, 41.

Contribution from the Department of Chemistry, Simon Fraser University, Burnaby, BC, Canada V5A 1S6

^{51}V NMR Investigation of the Interactions of Vanadate with Hydroxypyridines and Pyridinecarboxylates in Aqueous Solution

Bruno Galeffi and Alan S. Tracey*

Received June 29, 1988

The condensation of vanadate with salicylate, with pyridine, and with a variety of hydroxypyridines and pyridinecarboxylates in aqueous solution has been studied by using ^{51}V nuclear magnetic resonance spectroscopy. Vanadium atom, ligand, and hydrogen ion concentration studies have been carried out. Compared with the other ligands, pyridine and 3-hydroxypyridine undergo comparatively weak interactions with vanadate. 2-Hydroxybenzoate (salicylate) and 2-hydroxy-3-pyridinecarboxylate (2-hydroxynicotinate) react only weakly as chelating ligands to give products that appear to have octahedral symmetry. No evidence for condensation of vanadate between the hydroxyl and the nitrogen of 2-hydroxynicotinate was obtained. 2-Pyridinecarboxylate (picolinate) proved to be a good chelating agent to form a mixture of mono- and bis(ligand) species of apparent octahedral coordination. A further mono(ligand) product that was tentatively assigned a pentacoordinate coordination was also formed. 3-Hydroxy-2-pyridinecarboxylate (3-hydroxypicolinate) formed a complex mixture of products, with condensation of vanadate between the nitrogen and carboxylate and possibly between the carboxylate and the hydroxyl group occurring. pH studies allowed the proton stoichiometry for the various condensations to be obtained. Formation constants for the various condensation products from specified reactants have been obtained and are reported in this study.

Introduction

The aqueous chemistry of vanadium oxyanions has, over the past few years, become an area of expanding interest. There is a considerable amount of work which indicates that vanadium is an essential element.[1,2] Vanadium is extracted from seawater and concentrated to molar concentrations by ascidians, which store it as a V(III) derivative.[3] Vanadium-containing enzymes are found in various seaweeds where they are utilized for the formation of halogenated products.[2,4,5] Vanadium is also found in the enzymes of some nitrogen-fixing bacteria.[6] Furthermore, vanadate is a potent inhibitor of various enzymes and, similarly, a strong activator of a variety of others. Apparently, some of this function derives from the ability of vanadate (V(V)) (and perhaps vanadyl (V(IV))) to act as a phosphate analogue and, as such, vanadate provides a convenient probe for the investigation of mechanisms of enzyme action.

When in water, but dependent on pH, vanadate undergoes condensation reactions to form a variety of oligonuclear products including the dimer, tetramer, and decamer.[7] In the presence of aliphatic alcohols a rapid and reversible condensation occurs to provide tetrahedrally coordinated esters.[8] From water and

(1) Ramasarma, T.; Crane, F. L. *Curr. Top. Cell. Regul.* **1981**, *20*, 247-301.
(2) Erdmann, E.; Werdan, K.; Krawietz, W.; Schmitz, W.; Scholz, H. *Biochem. Pharm.* **1984**, *33*, 945-950.
(3) Kustin, K.; McLeod, G. C.; Gilbert, T. R.; Briggs, Le B. R., 4th *Struct. Bonding* **1983**, *53*, 139-160.
(4) Wever, R.; de Boer, E.; Plat, H.; Krenn, B. E. *FEBS Lett.* **1987**, *216*, 1-3.
(5) de Boer, E.; Boon, K.; Wever, R. *Biochemistry* **1988**, *27*, 1629-1635.
(6) Hales, B. J.; Case, E. E.; Morningstar, J. E.; Dzeda, M. F.; Mauterer, L. A. *Biochemistry* **1986**, *25*, 7251-7255.
(7) Pope, M. T.; Dale, B. W. *Rev. Chem. Soc.* **1968**, *22*, 527-548.
(8) Gresser, M. J.; Tracey, A. S. *J. Am. Chem. Soc.* **1985**, *107*, 4215-4220.

0020-1669/89/1328-1726$01.50/0